



ELSEVIER

# The effect of ion implantation of Ar on the aqueous corrosion resistance of Zr-4 alloy

Jinghao He<sup>\*</sup>, Xinde Bai, Chunlai Ma, Heming Chen

*Department of Materials Science and Engineering, Tsinghua University, Beijing 100084, China*

Received 16 June 1994; revised form received 30 November 1994

## Abstract

The effect of ion implantation on the aqueous corrosion resistance of Zr-4 in deaerated 1N H<sub>2</sub>SO<sub>4</sub> was studied with the potentiokinetic technique. The Zr-4 alloy was bombarded with  $5 \times 10^{14}$ – $2 \times 10^{16}$  Ar/cm<sup>2</sup> of 190 keV. It was found that the passive current density of Zr-4 decreases with increasing implantation dose. Photoelectrochemical results show that the ion implantation of Ar in Zr-4 raises the flatband potential of its passive film. AES was employed to analyze the surface of the passive film of Zr-4. The decrease in passive current density may be attributed to a thickening oxide layer on Zr-4 and a decrease in concentration of oxygen vacancies in its passive film.

## 1. Introduction

Zr-4 has been used extensively as fuel cladding and core structural material in light water reactors (LWRs) due to its low thermal neutron capture cross section, good corrosion resistance, adequate mechanical properties, and high thermal conductivity [1]. In reactors, Zr-4 is irradiated by neutrons, especially fast neutrons, which results in radiation damage and affects the corrosion process. Ion implantation is not only an interesting technique for modifying materials but also for simulating radiation damage. Many papers concentrated on modifying materials by adding other elements, but few papers referred to the effect of ion implantation damage on the corrosion process [2–4]. It is evident that the high concentration of defects produced by ion implantation is important to the corrosion behavior; however, this problem has not been investigated extensively.

In this paper, the effect of ion implantation damage on the polarization behavior of Zr-4 in 1N H<sub>2</sub>SO<sub>4</sub> at room temperature was studied with the potentiokinetic technique. Ar as bombarding ion was chosen in order to produce ion implantation damage without doping, because Ar is an inert gas element. To characterize the effect of ion implantation defects on the corrosion process, the photoelectrochemical method was applied to determine the flatband potential of passive films on implanted and nonim-

planted Zr-4. The flatband potential was considered to correlate to the defect structure of a passive film. In addition, AES was employed to analyze the surface of passive films of nonimplanted and implanted Zr-4.

## 2. Experimental procedure

The samples were machined from a plate of Zr-4, completely recrystallized by vacuum annealing, to about 12.0 mm × 12.0 mm length. The composition of Zr-4 is shown in Table 1. Samples were abraded with 400, 600 and 800 grit SiC and rinsed with deionized water before proceeding to the finer SiC grit. Then, they were degreased with acetone and ethanol and rinsed with deionized water.

Different conditions of ion implantation were arranged to study their influence on the aqueous corrosion of Zr-4. The samples were bombarded with  $5 \times 10^{14}$ – $2 \times 10^{16}$  Ar/cm<sup>2</sup> of 190 keV at room temperature or at liquid nitrogen temperature. The beam current density of Ar was 1.56 μA/cm<sup>2</sup>, and the pressure during ion implantation was  $1.33 \times 10^{-3}$  Pa.

The polarization curves were measured with the potentiokinetic technique in a conventional three electrode setup. The voltage sweep rate was 0.5 mV/s. The Zr-4 samples were placed as working electrodes. The counter electrode was made of platinum, and a standard calomel electrode served as a reference electrode. The electrolyte was 20°C 1N H<sub>2</sub>SO<sub>4</sub> deaerated with N<sub>2</sub> for an hour before the measurement.

The photoelectrochemical experiments were carried out by irradiating immersed samples with short-time pulses of

<sup>\*</sup> Corresponding author, Tel. +86 25 52451/61144, fax +86 25 62768.

Table 1  
Composition of Zr-4 alloy

Element	Content
Zr	base
Sn	1.4%
Fe	0.23%
Cr	0.1%
Ni	60 ppm
Al	< 14 ppm
Ti	< 14 ppm
Co	< 14 ppm
Mn	< 14 ppm
Mg	< 14 ppm
Pb	< 14 ppm
W	< 14 ppm
Mo	< 20 ppm
Cu	< 20 ppm
Si	< 50 ppm
Cl	< 20 ppm
C	< 100 ppm
N	< 30 ppm
O	< 900 ppm
H	< 10 ppm
Hf	< 100 ppm
B	< 0.5 ppm
Cd	< 0.5 ppm

white light from a 500 W xenon arc lamp. After the potentiokinetic tests the potential was ramped to the highest value, and then lowered at a sweep rate of 0.5 mV/s, while the sample was periodically irradiated with pulsed white light. The light shines from the xenon arc lamp through a water pool, a lens and a quartz window onto the sample immersed in the sulfuric acid. After about 20 seconds, the light was blocked off, returning the sample to the dark. The photocurrent was measured as the difference between the corrosion current with and without illumination, respectively. By comparing the positive photocurrent with the negative one, the zero photocurrent whose potential corresponds to the flatband potential of a passive film can be determined [5,6].

AES analyses were carried out in a Perkin Elmer PHI-60 spectrometer in order to obtain the thickness and oxygen concentration of passive films of implanted and nonimplanted Zr-4.

### 3. Experimental results

Fig. 1 shows the polarization curves of Zr-4 under different conditions of ion implantation. The common trend is that the ion implantation results in a decrease in passive current density of Zr-4 in 1N H<sub>2</sub>SO<sub>4</sub>. The higher the implantation dose, the smaller the passive current density. In addition, the passive current density of Zr-4 implanted with  $1 \times 10^{16}$  Ar/cm<sup>2</sup> of 190 keV at liquid

nitrogen temperature is higher than that at room temperature. After ion implantation, the color of the surface of the sample implanted with  $1 \times 10^{16}$  Ar/cm<sup>2</sup> of 190 keV at room temperature became shadow yellow, other implanted samples kept their original color.

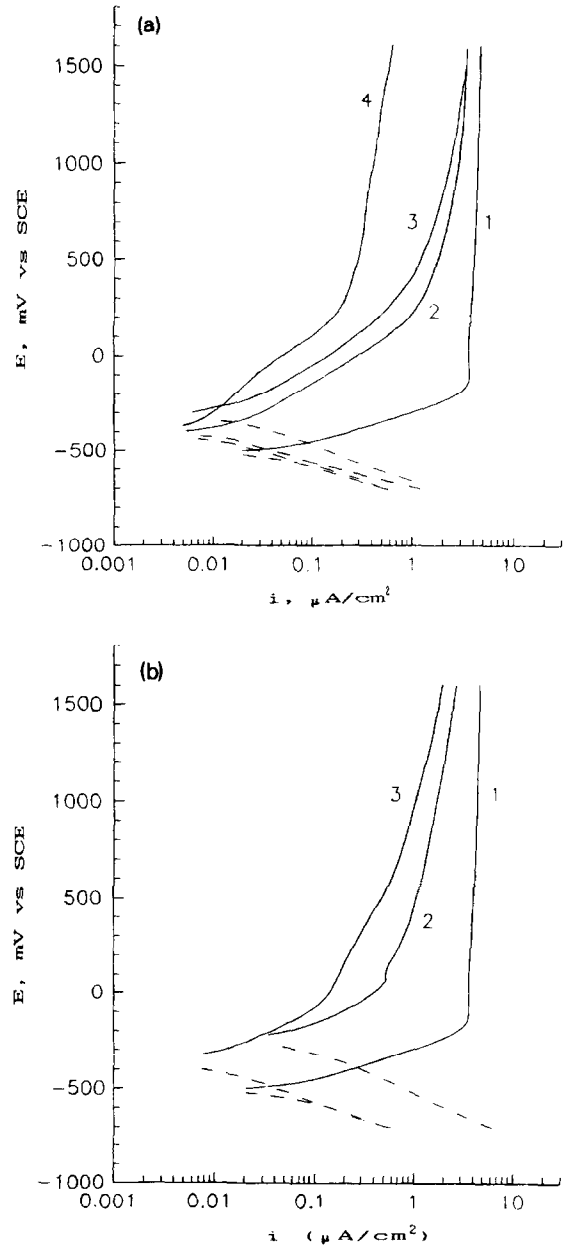


Fig. 1. Potential-current density curves of implanted and nonimplanted Zr-4 in 1N H<sub>2</sub>SO<sub>4</sub> deaerated with N<sub>2</sub>. (a): (1) nonimplanted Zr-4, (2) Zr-4 implanted at room temperature with  $5 \times 10^{14}$  Ar/cm<sup>2</sup>, (3)  $2.5 \times 10^{15}$  Ar/cm<sup>2</sup> and (4)  $1 \times 10^{16}$  Ar/cm<sup>2</sup> of 190 keV. (b): (1) nonimplanted Zr-4, (2) Zr-4 implanted at liquid nitrogen temperature with  $1 \times 10^{16}$  Ar/cm<sup>2</sup> and (3)  $2 \times 10^{16}$  Ar/cm<sup>2</sup> of 190 keV.

Fig. 2 shows the photoelectrochemical results of a passive film of Zr-4 after potentiokinetic tests. The flatband potential was determined by slowly decreasing the electrode potential and pulsing with white light to find the zero point of the photoeffect. The average between the potential of minimal positive photocurrent and that of

minimal negative photocurrent was used to detect the approximate flatband potential of a passive film. The experimental results reveal that the flatband potential of the passive film of nonimplanted Zr-4 is about 70 mV (SCE) and the ones implanted with  $1 \times 10^{16}$  Ar/cm<sup>2</sup> of 190 keV at liquid nitrogen temperature and at room tem-

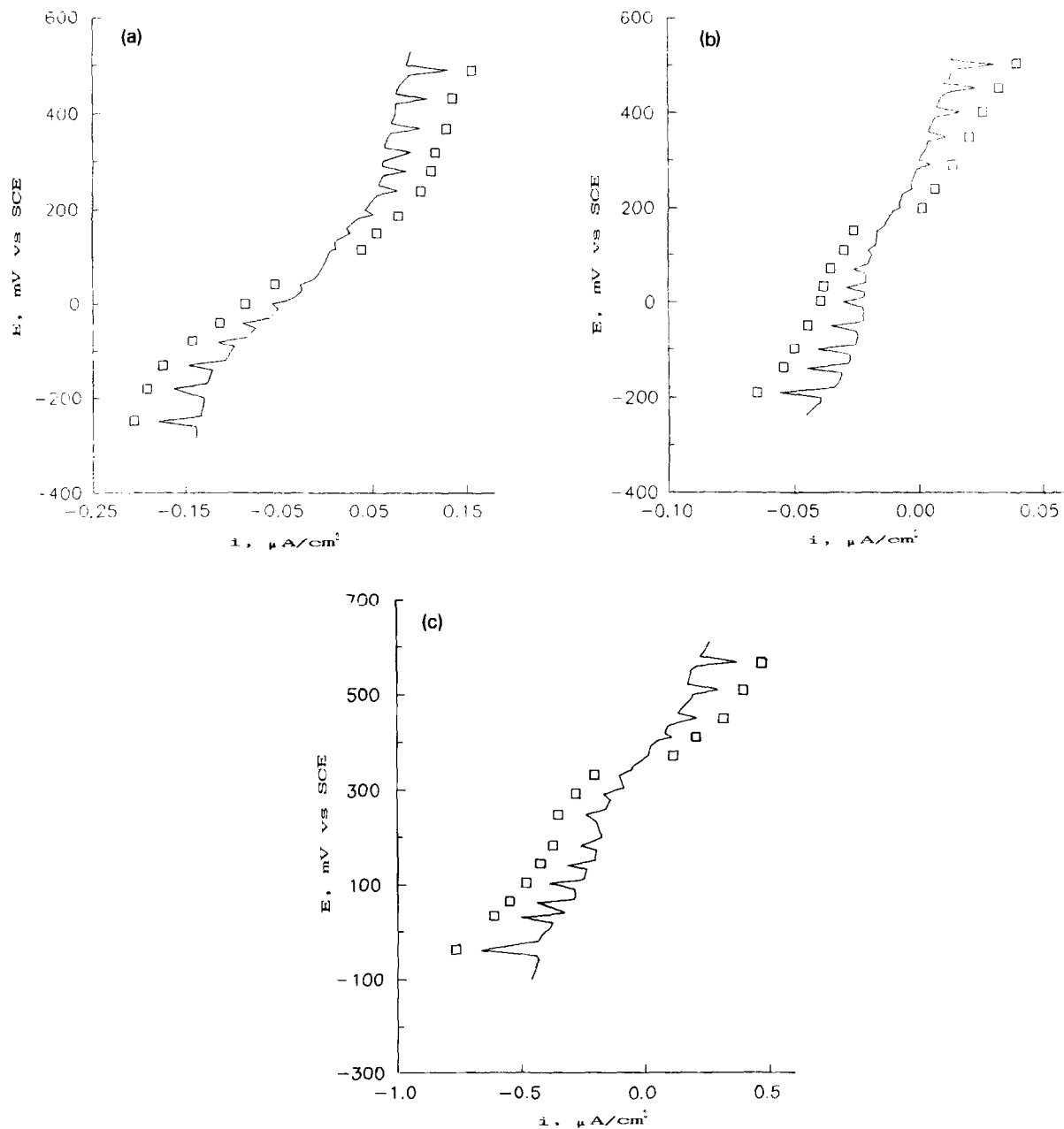


Fig. 2. Photoelectrochemical results. Note: the open squares represent illumination from a xenon arc lamp. (a): Passive film of nonimplanted Zr-4. (b): Passive film of Zr-4 implanted with  $1 \times 10^{16}$  Ar/cm<sup>2</sup> of 190 keV at liquid nitrogen temperature. (c): Passive film of Zr-4 implanted with  $1 \times 10^{16}$  Ar/cm<sup>2</sup> of 190 keV at room temperature.

perature are about 175 mV (SCE) and 350 mV (SCE), respectively. Therefore, it is concluded that implantation of Ar in Zr-4 alloy induces an increase in flatband potential of its passive film, though there is uncertainty because of noise in the measurement.

Fig. 3 shows AES analyses of passive films of nonimplanted and implanted Zr-4. It is obvious that, after polarization to the same potential in 1N H<sub>2</sub>SO<sub>4</sub>, the passive film of nonimplanted Zr-4 is almost as thick as those of films implanted with  $5 \times 10^{14}$  Ar/cm<sup>2</sup> of 190 keV at room temperature and  $2 \times 10^{16}$  Ar/cm<sup>2</sup> of 190 keV at liquid nitrogen temperature. However, the thickness of the passive film of Zr-4 implanted with  $1 \times 10^{16}$  Ar/cm<sup>2</sup> of 190 keV at room temperature is much greater than that of nonimplanted Zr-4. In addition, the oxygen concentration of the passive film implanted with  $1 \times 10^{16}$  Ar/cm<sup>2</sup> of 190 keV at room temperature is higher than that of the passive film of nonimplanted Zr-4; however, it can only be surmised that the one implanted with  $2 \times 10^{16}$  Ar/cm<sup>2</sup> of

190 keV at liquid nitrogen temperature is a bit higher than that of nonimplanted Zr-4 from AES analyses, because the difference in the oxygen concentration is so small (2–3%) that AES cannot detect it effectively and more precise surface analysis is needed to verify it.

#### 4. Discussion

Usually, ion implantation is beneficial to the formation of thin oxide film on metal surface [7,8]. When the sample of Zr-4 was implanted with  $1 \times 10^{16}$  Ar/cm<sup>2</sup> of 190 keV with a beam current density of  $1.56 \mu\text{A}/\text{cm}^2$  at room temperature, because of the uncooled metal surface, the deposition of ion implantation energy in Zr-4 causes a drastic increase in surface temperature, and this may induce a thermal oxidation at the pressure  $1.33 \times 10^{-3}$  Pa, which changed the surface color of the sample to shadow yellow, an interference color due to a thin oxide layer.

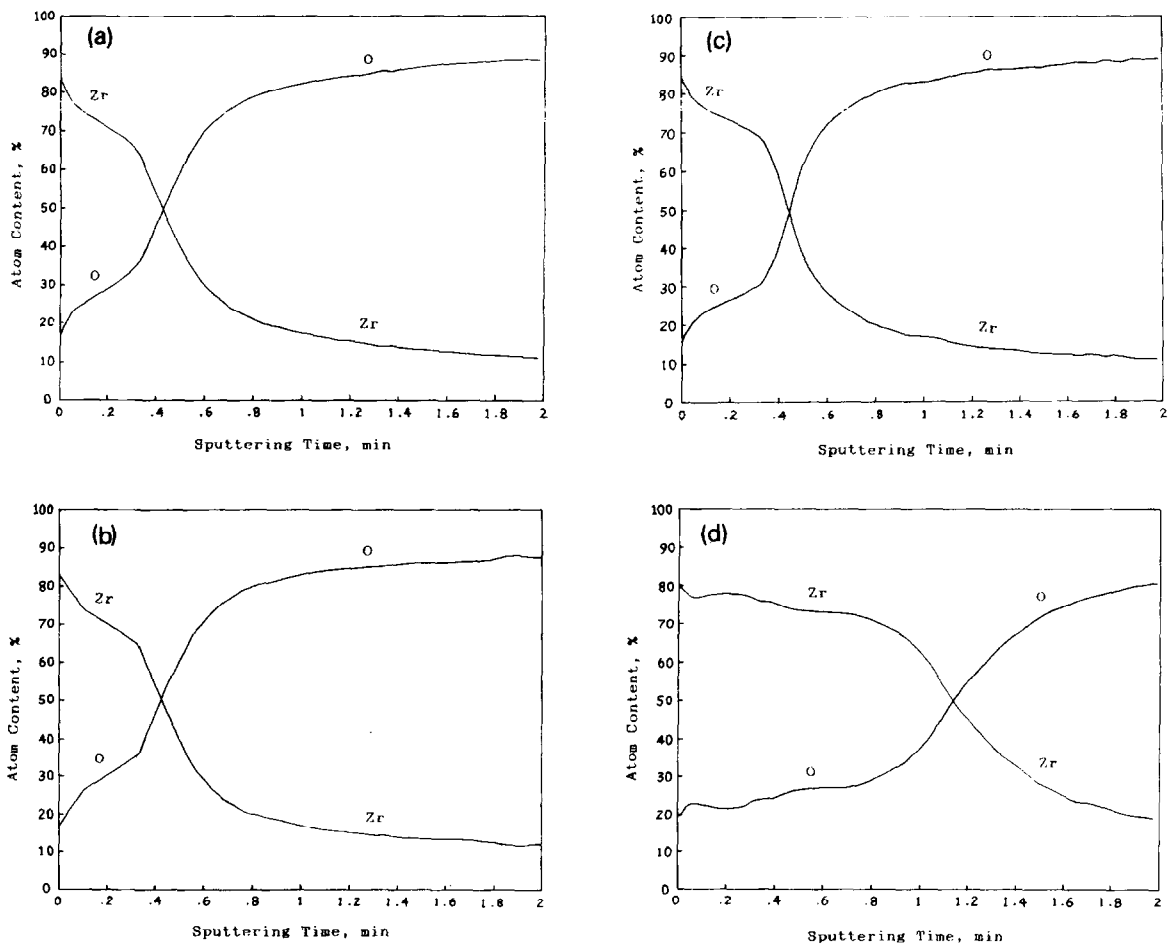


Fig. 3. The composition–depth analyses of passive films of implanted and nonimplanted Zr-4 by AES. (a): Passive film of nonimplanted Zr-4. (b): Passive film of Zr-4 implanted with  $5 \times 10^{14}$  Ar/cm<sup>2</sup> of 190 keV at room temperature. (c): Passive film of Zr-4 implanted with  $2 \times 10^{16}$  Ar/cm<sup>2</sup> of 190 keV at liquid nitrogen temperature. (d): Passive film of Zr-4 implanted with  $1 \times 10^{16}$  Ar/cm<sup>2</sup> of 190 keV at room temperature.

However, the surfaces of Zr-4 during implantation under the same beam current density with  $5 \times 10^{14}$  Ar/cm<sup>2</sup> of 190 keV at room temperature and  $2 \times 10^{16}$  Ar/cm<sup>2</sup> of 190 keV at liquid nitrogen temperature were respectively about room temperature and low temperature, because the deposition of ion implantation energy in Zr-4 is relatively small in the former case and the heat transfer is rapid in the latter case. Hence, the thermal oxidation of Zr-4 under these conditions was inhibited, and the surface kept its original color.

Thickening oxide film due to ion implantation reduces the passive current density of Zr-4 in 1N H<sub>2</sub>SO<sub>4</sub>, because the oxide film functions as a barrier. In addition, the large number of defects produced by ion implantation also influences the passivity of Zr-4. Since the passive films of Zr-4 implanted with  $5 \times 10^{14}$  Ar/cm<sup>2</sup> of 190 keV at room temperature and  $2 \times 10^{16}$  Ar/cm<sup>2</sup> of 190 keV at liquid nitrogen temperature are almost as thick as that of nonimplanted Zr-4, see AES composition–depth analyses, the difference in passive current density of these samples may result from a large number of radiation defects or Ar impurities.

Metal oxides composed of metal ions and oxygen ions can be classified as stoichiometric and nonstoichiometric oxides. Generally, most metal oxides are nonstoichiometric, and behave like semiconductors. Zirconium oxides have defects in the form of anion vacancies [9]. Excess electrons (quasi-free electrons) in oxides will maintain electroneutrality.

It must be noted that the flatband potential of the oxide is dependent on the defect content, which is a result of impurity ions, vacancies or nonstoichiometry of the oxide. From the photoelectrochemical results, the rise of the flatband potential, which corresponds to a lowering of the Fermi level, of a passive film formed on implanted Zr-4 may result from the higher oxygen concentration in a passive film, because Ar, an inert gas element, cannot offer and accept electrons which influence the Fermi level of a passive film of Zr-4. The defects caused by ion implantation result in a sharp increase of the affinity of the metal surface to oxygen, which facilitates the formation of a quantitative better protective film [4]. So, the passive film accommodates more oxygen ions and the excess oxygen ions probably occupy the original oxygen vacancies and induce a decrease in concentration of oxygen vacancies, which can be seen and surmised in AES analyses of passive films of Zr-4 implanted with  $1 \times 10^{16}$  Ar/cm<sup>2</sup> of 190 keV at room temperature and  $2 \times 10^{16}$  Ar/cm<sup>2</sup> of 190 keV at liquid nitrogen temperature. If so, the concentration of quasi-free electrons inevitably decreases to maintain electroneutrality and results in the lowering of the Fermi level of the passive film. It may therefore be concluded that the flatband of a passive film of Zr-4 under different implantation conditions reflects its concentration of oxygen vacancies.

The variation of oxygen vacancy concentration has an

influence on the migration of oxygen ions, and thus on the corrosion current. According to the point defect model (PDM) [10–12], the steady-state current is related to the fluxes of cation vacancies and oxygen vacancies through the passive film and can be expressed as

$$I_{SS} = F \left[ \delta J_M - 2 \left( \frac{\delta}{\chi} \right) J_O \right], \quad (1)$$

where  $F$  is Faraday's constant (96487 C/mol) and  $J_M$  and  $J_O$  are the fluxes of cation and oxygen vacancies, respectively, at the metal/barrier film interface.  $\delta$  is the valence of the metal ion dissolved in solution from an oxide film.  $\chi$  is the valence of the metal ion in the oxide film. It is known that oxygen ions migrate into an oxide film in the anodic oxidation of Zr through the Marker experiment; however zirconium ions do not migrate [13]. In Zr-4, the content of Sn, Fe and Cr is very low, so the passive film of Zr-4 can be regarded as a zirconium oxide and it is reasonable to assume  $J_M = 0$ . Therefore, the steady-state passive current  $I_{SS}$  is only dependent on and proportional to  $J_O$ . Moreover, the flux of oxygen vacancies may be written in approximate form as [10]

$$J_O = -D_O \left( \frac{dC_O}{dx} \right) - 2KD_O C_O, \quad (2)$$

where  $C_O$  is the concentration of oxygen vacancies.  $D_O$  denotes the diffusion coefficient of oxygen vacancies.  $x$  is the distance to the film/solution interface.  $K = EF/RT$ , where  $E$  is the mean electric field strength  $E = V_{OX}/L$ .  $V_{OX}$  is the voltage applied on the passive film and  $L$  is the thickness of the passive film.  $R$  and  $T$  have their usual meaning. Combination of Eqs. (1) and (2) and formulas about  $K$  and  $E$  therefore yields

$$I_{SS} = 2FD_O \left( \frac{\delta}{\chi} \right) \left[ \left( \frac{dC_O}{dx} \right) + 2 \frac{FV_{OX}}{RTL} C_O \right]. \quad (3)$$

According to Eq. (3), if the thickness of the passive films is the same, the decrease in concentration of oxygen vacancies may induce a decrease of  $I_{SS}$ . Also, an increase in the thickness of the passive film reduces  $I_{SS}$ . This can explain why the passive current density of Zr-4 implanted with  $1 \times 10^{16}$  Ar/cm<sup>2</sup> of 190 keV at liquid nitrogen temperature is much smaller than that of nonimplanted Zr-4 and much higher than that of Zr-4 implanted with  $1 \times 10^{16}$  Ar/cm<sup>2</sup> of 190 keV at room temperature.

The above analyses show that the ion implantation thickens the oxide layer, which forms a barrier, and induces a decrease in the passive current density. Additionally, the decrease in concentration of oxygen vacancies caused by ion implantation may reduce the flux of oxygen vacancies and the passive current density. However, ion implantation is a complicated process interacting with materials and has many effects on the corrosion resistance. For example, ion implantation with Ar enables the formation of interstitial and substitutional solid solutions of inert

gas with metals, which, firstly, occupy active adsorption centers and, secondly, act as barriers for diffusion of gases such as hydrogen and oxygen, oxygen-containing gases, etc., into the metal volume, because such barrier layers have an increased binding force compared with the bulk [4]. Besides the effects of the thickening of the oxide layer and the decrease of the concentration of oxygen vacancies by ion implantation, other effects need further studying.

## 5. Conclusions

Under the above experimental conditions, we can come to the following conclusions:

(1) Ion implantation of Ar in Zr-4 reduces its passive current density in a 1N H<sub>2</sub>SO<sub>4</sub> solution at room temperature. The higher the implantation dose, the smaller the passive current density.

(2) Ion implantation of Ar in Zr-4 raises the flatband potential of its passive film formed in 1N H<sub>2</sub>SO<sub>4</sub>.

(3) Ion implantation of Ar in relatively high dose ( $1 \times 10^{16}$  Ar/cm<sup>2</sup>) at room temperature thickens the oxide layer of Zr-4 obviously.

(4) The effect of ion implantation of Ar on the aqueous corrosion resistance of Zr-4 may be explained as: (a) the oxide layer caused by ion implantation functions as a barrier and reduces the passive current density. (b) ion implantation defects may stimulate the accommodation of

oxygen ions in Zr-4 and result in a lower concentration of oxygen vacancies in the passive film, which reduces the passive current density.

## References

- [1] S. Kass, in: Corrosion of Zirconium Alloys, ASTM STP 368 (STM, Philadelphia, 1964) p. 3.
- [2] H. Ferber, H. Kasten, G.K. Wolf, W.J. Lorenz, H. Schweickert and H. Folger, Corros. Sci. 20 (1980) 124.
- [3] Wei Tian, Weiping Cai, Jun Li, and Run Wu, Mater. Sci. Eng. A 116 (1989) 15.
- [4] T.D. Radjabov, Vacuum 38 (1988) 979-995.
- [5] T.D. Berleigh and R.M. Latanision, J. Electrochem. Soc. 134 (1987) 135.
- [6] T.D. Berleigh and R.M. Latanision, Corrosion 43 (1987) 471.
- [7] Ashworth, W.A. Grant, R.P.M. Procter and T.C. Wellington, Corros. Sci. 16 (1976) 775.
- [8] G. Dearnaley and P.D. Goode, Nucl. Instr. and Meth. 189 (1981) 117.
- [9] Heming Chen, Chunlai Ma and Xinde Bai, in: Corrosion and protection of nuclear materials (Atomic Energy Press, Beijing, 1984) p. 23. in Chinese.
- [10] D.D. Macdonald and M. Urquidi-Macdonald, J. Electrochem. Soc. 137 (1990) 2395.
- [11] D.D. Macdonald and S.I. Smedley, Electrochim. Acta 35 (1990) 1949.
- [12] D.D. Macdonald, S.R. Biaggio and Herking Song, J. Electrochem. Soc. 139 (1992) 170.
- [13] Z.C. Zhang, ME dissertation of Tsinghua University (1986).